

QCD Scattering Processes with Hard Gluon Emission

Z. Kunszt

Deutsches Elektronen-Synchrotron DESY, Notkestrasse 85, D-2000 Hamburg 52, Federal Republic of Germany

E. Pietarinen

Institut für Theoretische Kernphysik der Universität Karlsruhe, Kaiserstrasse 12, D-7500 Karlsruhe, Federal Republic of Germany

Received 8 June 1979

Abstract. $2 \rightarrow 3$ QCD scattering processes are studied in kinematical regions which are free from infrared and mass singularities. Anomalously large hard gluon emission corrections are found to gluon-gluon annihilation $gg \rightarrow q\bar{q}$. It is pointed out that in a kinematical region where azimuthal angle correlations of large transverse momentum π^0 's have been measured at ISR, the 3-jet production rate is large and the contribution of the subprocess $gq \rightarrow ggq$ is greater than the contributions from quark-quark scattering $qq \rightarrow qqg$.

There is now considerable experimental evidence that QCD hard scattering and annihilation processes can successfully describe e.g. muon pair production, four jet structure for large p_{\perp} events and quarkonium production [1, 2]. In this approach, to leading order in the QCD running coupling constant α_s , the physical cross sections are calculated from the cross sections of the pointlike processes ($q\bar{q} \rightarrow \mu^+\mu^-$, $q\bar{q} \rightarrow c\bar{c}$, 2-2 scattering reactions, etc.) folded with parton distribution and fragmentation functions. This procedure now has firmer theoretical foundation since it has been proved that mass singularities can be factorized in QCD [3].

There are, however, several problems, as well. The transverse momentum smearing required for large p_{\perp} events appears to be too large, the value of $\langle \mathcal{P}_{\text{out}} \rangle$ is higher than the predicted one [2], there is a considerable discrepancy between the leading order QCD predictions and the measured cross section value for charm production etc. [4].

In the present range of energies, $\alpha_s(Q^2)$ is not sufficiently small to make the lowest order approximation as precise as needed. Higher order corrections may become important leading to non-negligible effects or even qualitatively new phenomena. One may argue that the problems encountered above can be remedied, at least partly, by adding to the

Born diagrams the first order QCD corrections. An example has been provided, e.g. by the p_{\perp} distribution of the μ -pair of the Drell-Yan process [5]. Corrections to single particle distributions are given by hard gluon bremsstrahlung and one-loop diagrams. A complete study of the $1/\log p_{\perp}$ corrections have been carried out only for the Drell Yan process [6]. We have, however, several physical quantities like p_{\perp} distribution of heavy quarkonium, 3 jet production, azimuthal correlations and transverse thrust distributions which even in Born approximation are determined by the $2 \rightarrow 3$ scattering processes, since loop corrections vanish due to kinematical reasons.

In this paper we study $2 \rightarrow 3$ QCD scattering processes in kinematical regions which are free from infrared and mass singularities. First we discuss the somewhat unphysical quantities: pointlike parton cross sections. Such a discussion appears us to be useful since the expressions obtained for the cross sections are too long to be suitable for publication. The large variety of possible applications of the $2 \rightarrow 3$ scattering processes assumes a clear understanding of the properties of the pointlike hard scattering cross sections, as well. We also give a short discussion of the 3-jet cross sections¹, obtained by folding the pointlike cross sections with parton distribution functions.

Here we present results for the following processes:

$$\begin{aligned}
 qQ &\rightarrow qQG \text{ (a)} & Gq &\rightarrow GGq \text{ (e)} \\
 q\bar{Q} &\rightarrow q\bar{Q}G \text{ (b)} & \bar{q}q &\rightarrow GGG \text{ (f)} \\
 q\bar{q} &\rightarrow Q\bar{Q}G \text{ (c)} & GG &\rightarrow GQ\bar{Q} \text{ (g)} \\
 Gq &\rightarrow Q\bar{Q}q \text{ (d)}
 \end{aligned}
 \tag{1}$$

¹ 3-jet cross sections have been studied in the quark fusion model in [7], and in QCD hard scattering model using the subprocess $q+q \rightarrow q+q+g$ in [8]

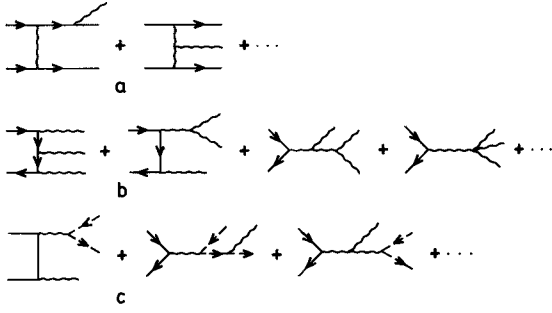


Fig. 1a–c. Some typical Feynman diagrams describing hard gluon emission amplitudes: $q\bar{q} \rightarrow q\bar{q}G$ (a), $q\bar{q} \rightarrow GGG$ (b), ghost contributions to $q\bar{q}GGG$ (c)

where q and Q denote quarks having different flavours and G denotes a gluon.²

The $2 \rightarrow 3$ scattering processes can be classified into three subclasses, namely to four quark-one gluon, two quark-three-gluon and five gluon amplitudes. In the first case we have five or ten Feynman diagrams with unequal or equal flavour, respectively, the $2q3G$ amplitude is described by sixteen diagrams and the $5G$ amplitude is given by 25 diagrams. Some typical Feynman diagrams are given in Fig. 1.

The invariant squared matrix elements $|M_{ij}^2|$ were calculated with the computer program REDUCE [9]. The complexity of the calculation increases with the number of the gluon lines since, unlike in QED, in gluon polarization sums either we must sum over the physical helicities only or we have to use a covariant gauge and add the contributions of ghost diagrams. In the latter case the number of the Cutkosky diagrams to be calculated are 25 for $QqQqG$, 281 for $GGGqq$ and 1006 for the five gluon amplitudes.

The algebraic calculation performed in a covariant gauge was checked by an entirely independent numerical program using helicity projectors. Such a check ensures correct signs of quark–gluon, gluon–gluon and ghost–gluon couplings and the colour traces.

We have calculated the matrix elements with running coupling constant $\alpha_s(E_{\perp}^2/\Lambda^2)$, where

$$E_{\perp} = |\not{k}_{1\perp}| + |\not{k}_{2\perp}| + |\not{k}_{3\perp}| \quad (2)$$

with $\Lambda = 0.5$ GeV and flavour number $N_F = 5$.

In order to avoid infrared and mass singularities the values of the total cross sections have been calculated with transverse momentum, polar angle and acoplanarity cut-offs. Let us assume that two of the final particles would be observed in a cylindrical detector with polar angle aperture Θ_c . If we demand that the transverse momentum of the observed

“jets” is larger than a cut-off value \not{k}_{\perp}^c and the angles³ between the transverse momenta of the two particles are in the range $180 - \phi_c \geq \phi \geq \phi_c$, then we cut off the soft and collinear configurations. For the perturbation theory to be meaningful of the $2 \rightarrow 2$ scattering cross sections with the same polar angle cut Θ_c ought to be larger.

In Table I we give the values of the total cross sections for $2 \rightarrow 2$ scattering at $\sqrt{s} = 20$ GeV, for several Θ_c cuts as well as the values of the total cross sections for the $2 \rightarrow 3$ scattering processes with the same values of Θ_c , with additional cuts on the transverse momenta of the “observed jets” $\not{k}_{\perp}^c > 2.5$ GeV and on azimuthal angles⁴ $\phi_c = \pi/8, \pi/4$.

The relative magnitude of the hard gluon bremsstrahlung cross sections with respect to the $2 \rightarrow 2$ scattering cross sections can be enhanced or suppressed by changing the magnitude of the cuts, e.g. changing the value of ϕ_c from $\pi/8$ to $\pi/4$ or the value of \not{k}_{\perp}^c from 2.5 GeV to 5 GeV, the hard gluon cross sections become smaller with a factor of ≈ 3 , in the average.

The critical value of ϕ_c and E_c where radiative corrections become exceedingly large (30–40%) may be interpreted as a measure of “jet broadening” of the jets produced in hadron–hadron collisions. This is further illustrated by Fig. 2, where cross sections of three different hard scattering processes are plotted as a function of δ and ε .⁵

As we can see from Fig. 2 and Table 1 in general, the hard gluon emission processes give 20%–30% effects with $\varepsilon = 0.2$, $\delta = 0.2$ –0.3 as compared with the leading order cross sections, similarly to jets produced in e^+e^- annihilation. There is, however, a very interesting exception: $GG \rightarrow Gq\bar{q}$. In this case the magnitude of the cross section with respect to the leading order cross section is 5–6 time larger than the same ratio for all the other processes. This exceptional value of the hard gluon emission, however, does not mean necessarily that its perturbative calculation is meaningless. It is a consequence of the anomalously large ratio of the cross sections in case of the $2 \rightarrow 2$ scattering $\sigma(qg \rightarrow qg)/\sigma(qg \rightarrow q\bar{q}) = 150$ –250. The process $GG \rightarrow Gq\bar{q}$ can also be interpreted as a “Dalitz-conversion” correction

³ $\pi - \phi$ is called in discussions of radiative corrections to Bhabha scattering as an “acoplanarity angle”. In order to further test our calculation we have changed the colour factors to QED values and then we could reproduce the cross section values published in [11] in Table 6 for Bhabha scattering

⁴ These cuts are not symmetric in the variables of the final particles. Table 1 gives the average value of the three possible pairings of the final “jets” as “observed jets”. The phase space integrations were made by a Monte Carlo method, and the numbers in Table 1 and 2 have 5–10% accuracy.

⁵ δ and ε denote the angle and energy cuts as proposed in [12]. All the angles between the three momenta of the final particles and the beam direction are required to be larger than δ , and the energy fraction carried by any of the final jets is required to be larger than ε .

² Cross sections with equal flavour ($q = Q$) differ from the ones with $q \neq Q$ by 5–10%. The cross section of the process $GG \rightarrow GGG$ is presently being calculated

to elastic gluon–gluon scattering. In this comparison the cross section of the process $GG \rightarrow Gq\bar{q}$ is small.⁶ It might be that we have a situation which has resemblance with the QED process $e^+e^- \rightarrow e^+e^-\mu^+\mu^-$, where at high energies $\sigma(e^+e^- \rightarrow e^+e^-\mu^+\mu^-) > \sigma(e^+e^- \rightarrow \mu^+\mu^-)$, but the cross section $\sigma(e^+e^- \rightarrow e^+e^-\mu^+\mu^-)$ can be safely calculated in perturbation theory. If we accept this point of view, the contribution of this process may be important in describing charm and quarkonium production.

We have calculated the cross sections also at higher energies (100, 150, 200 GeV), and we have found that keeping $\theta_c, \phi_c, \not{p}_{\perp c}/\sqrt{s}$ fixed, the pattern of the relative importance of different subprocesses and the ratio $\sigma(3\text{ jet})/\sigma(2\text{ jet})$ remained practically the same. This also indicates that if factorization of the collinear and infrared singularities holds also for transverse momentum distribution then instead of \not{p}_{\perp} we must use $x_{\perp} = 2\not{p}_{\perp}/\sqrt{s}$ [13].

The most interesting question is whether the sizeable 3-jet corrections will manifest themselves also in physical processes. A partial answer is given in Table 2, where we give cross sections folded with parton distribution functions for proton–proton collisions with $\sqrt{s} = 52$ GeV, $\not{p}_{\perp c} = 1.5$ or 2.5 GeV and for the

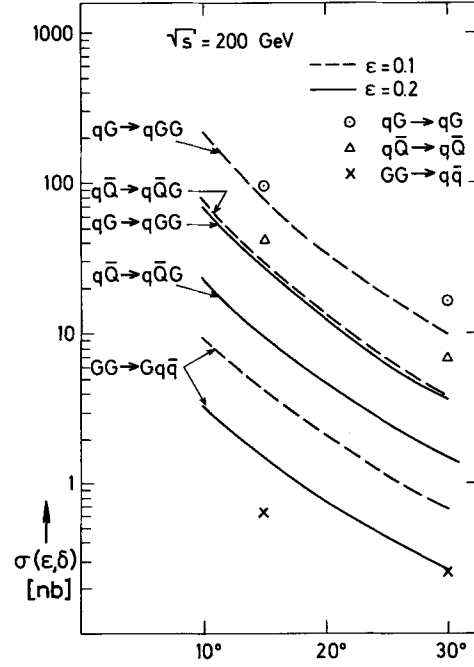


Fig. 2. Cross sections for subprocesses $qg \rightarrow qgq, q\bar{q} \rightarrow q\bar{q}g, gg \rightarrow gq\bar{q}$ as a function of δ at $\epsilon = 0.1$ and 0.2 . The cross section values for the corresponding elastic processes are also indicated.

Table 1. Cross section values in nanobarns for seven different $2 \rightarrow 3$ scattering subprocesses, with polar angle, azimuthal angle and \not{p}_{\perp} cuts, $\theta_c, \phi_c, \not{p}_{\perp}^{\text{vis}}$ at incoming energy $\sqrt{s} = 20$ GeV. The numbers in parentheses are the values of the cross sections for the corresponding $2 \rightarrow 2$ processes with the same value of θ_c .

$qQ \rightarrow qQG$ (nbarn)	$q\bar{Q} \rightarrow q\bar{Q}G$ (nb)	$q\bar{q} \rightarrow Q\bar{Q}G$ (nb)	$Gq \rightarrow Q\bar{Q}q$ (nb)	$Gq \rightarrow GGq$ (nb)	$GG \rightarrow Gq\bar{q}$ (nb)	$q\bar{q} \rightarrow GGG$ (nb)	θ_c	Comments
4500 (1.4 × 10 ⁴)	4600 (1.4 × 10 ⁴)	32 (53)	107	1.2 × 10 ⁴ (3.2 × 10 ⁴)	530 (200)	150 (700)	15°	$\phi_c = \pi/8$
1200 (2000)	1240 (2000)	20 (41)	38	3000 (4800)	180 (70)	85 (255)	30°	$\not{p}_{\perp}^{\text{vis}} >$
300 (630)	343 (630)	11 (29)	13	830 (1600)	65 (32)	41 (115)	45°	$\not{p}_{\perp}^{\text{vis}} > 2.5$ GeV
75 (250)	91 (250)	4.6 (18)	.93	240 (500)	21 (15)	15 (54)	60°	
1400 (1.4 × 10 ⁴)	1500 (1.4 × 10 ⁴)	15 (53)	41	3800 (3.2 × 10 ⁴)	200 (200)	158 (700)	15°	$\phi_c = \pi/4$
450 (2000)	500 (2000)	9.2 (41)	16	1200 (4800)	80 (70)	35 (255)	30°	$\not{p}_{\perp}^{\text{vis}} > 2.5$ GeV
32 (630)	41 (630)	4.8 (29)	5.6	350 (1600)	27 (32)	17 (115)	45°	
5.5 (250)	7.6 (250)	2.0 (18)	1.8	100 (500)	1.9 (15)	6.6 (54)	60°	

Table 2. Contributions of seven different QCD $2 \rightarrow 3$ subprocess to 3-jet production in proton–proton collisions at energy $\sqrt{s} = 52$ GeV, with azimuthal angles $\phi_c < 7\pi/8$. The values in parenthesis are the cross section values of the contribution of the corresponding $2 \rightarrow 2$ subprocesses with the same value of transverse energy

$qQ \rightarrow qQG$ (nbarn)	$q\bar{Q} \rightarrow q\bar{Q}G$ (nb)	$q\bar{q} \rightarrow Q\bar{Q}G$ (nb)	$Gq \rightarrow Q\bar{Q}q$ (nb)	$Gq \rightarrow GGq$ (nb)	$GG \rightarrow Gq\bar{q}$ (nb)	$q\bar{q} \rightarrow GGG$ (nb)	$\not{p}_{\perp}^{\text{vis}}$ (GeV)	Transverse energy (GeV)	E_{\perp}
1900. (2370.)	320. (580.)	14. (42.)	260.	3360. (5600.)	120. (68.)	9.4 (35.)	1.5	8 < E _⊥ < 10	
255.	40.	1.5	24.	380.	12.	.87	2.5	8 < E _⊥ < 10	
490. (620)	50. (110)	2.4 (8.5)	37.	540. (1090)	14. (10.)	1.5 (6.8)	1.5	10 < E _⊥ < 12	
200.	26.	1.3	20.	270.	7.3	.8	2.5	10 < E _⊥ < 12	

⁶ The value of the cross section $\sigma(gg \rightarrow gg)$ at $\sqrt{s} = 20$ GeV, $\theta = 15^\circ$ is equal to $\sim 73 \mu\text{barn}$

transverse energy ranges $E_{\perp} = 8-10, 10-12 \text{ GeV}^7$. The main features of this application can be summarized as follows:

i) Since the parton distribution functions are steeply changing with $\tau = x_1 x_2$, the three jet contributions in a given data sample can be enhanced or suppressed with suitable cuts. In particular, we have found that if we apply transverse momentum (or energy) and azimuthal cuts only, the ratio of the 3-jet \rightarrow 2-jet contributions is suppressed by factor 3–10 as compared with the ratio of the parton cross sections. This is explained in part by kinematical effects and in part by the properties of the parton distribution functions. In a physical hadron–hadron scattering process the main contributions come from the region where the energy \sqrt{s} of the hard scattering process is smallest. Further suppression is coming from the effective value of τ which is larger for the 3 jet processes than for the corresponding 2 jet processes. Folding with the distribution functions with p_{\perp} cuts contributions from large scattering angles are enhanced, which further reduces the 3 jet processes.

However, if the cross sections are calculated at an approximately fixed transverse energy E_{\perp} (as given in Table 2) with a relatively small p_{\perp} cut, the three mechanisms mentioned above become ineffective. An advantage of this kind of cut-off procedure is that it will enrich 3 jet events in the data.⁸ Indeed it was observed experimentally [15] that the azimuthal angle distributions of two large transverse momentum π^0 produced in proton–proton collisions at $\sqrt{s} = 53 \text{ GeV}$ at ISR become much flatter if the distribution is plotted at fixed transverse energy (and not only with some p_{\perp} cut).

In [9] it was argued that this is partly a consequence of the properties of the distribution functions, which enhance the back-to-back configuration if E_{\perp} is not fixed. We emphasize that in addition it is very essential that the relative importance of the 3-jet contribution is strongly enhanced⁹. If the transverse energy is not fixed (at a value relatively large compared to the p_{\perp} cut) the azimuthal distribution is mainly given by the smeared 2-jet contributions. At fixed E_{\perp} , however, the 3 jet contribution is revealed.

ii) As it is obvious from Table 2, the contribution of the gluon–quark scattering subprocess $gq \rightarrow gqg$ is larger than the contribution of $qq \rightarrow qqg$, in the kinematical region where the ISR measurement

has been performed ($\sqrt{s} = 62 \text{ GeV}$, $E_{\perp} = 8-10$, $\phi_e = 23^\circ$, $p_{\perp e} = 1.5 \text{ GeV}$). A quantitative comparison with the ISR data requires also the inclusion of quark and gluon fragmentation into π^0 . The details of such an analysis will be published elsewhere.

In conclusion we have shown that hard gluon emission process give 20% corrections in comparison with Born approximation for parton–parton scattering processes, similarly to the size of hard gluon bremsstrahlung effects calculated for e^+e^- annihilation and lepto-production. Anomalously large corrections have been found to the gluon–gluon annihilation $gg \rightarrow g\bar{q}$. We pointed out that in the kinematical region where azimuthal angle correlations of large transverse momentum π^0 's have been measured at ISR, the 3 jet production rate is large and the contribution of the $gg \rightarrow gqg$ subprocesses is larger than the contribution of quark–quark scattering $qq \rightarrow qqg$.

Acknowledgement. We are grateful to E. Reya for numerous valuable discussions. We also thank DESY for hospitality. E.P. acknowledges the partial support by the Academy of Finland.

References

1. M. Jacob, P.V. Landshoff: Phys. Rep. **48C**, No. 4 (1978)
2. R.P. Feynman, R.D. Field, G.C. Fox: CALT-68-651 (1978)
3. C.T. Sachrajda: Phys. Lett. **76B**, 100 (1978);
W. Furmanski: Cracow Univ. preprint TPJU = 10/78;
R. Ellis, H. Georgi, M. Machacke, H. Politzer, G. Ross: CALT 68–684 (1978);
J. Kripfganz: Leipzig preprint KMU-HEP-78-12;
D. Amati, R. Petronzio, G. Veneziano: CERN TH-2527 (1978)
4. D. Drijard et al.: submitted to Phys. Lett. **B** (1979)
5. L.M. Jones, H.W. Wyld: Phys. Rev. **D17**, 2332 (1978)
H. Fritzsche, K.H. Streng: Phys. Lett. **72B**, 385 (1978);
M. Glück, E. Reya: Phys. Lett. **79B**, 4 (1978);
B.L. Combridge: CERN preprint TH 2574 (1978);
H. Georgi, M. Machaczek, D. Nanopoulos, S. Glashow: Ann. of Phys. **114**, 273 (1978)
6. F. Halzen: Invited talk at the XIX International Conference on High Energy Physics, Tokyo, Japan (1978)
7. G. Altarelli, R. Ellis, G. Martinelli: MIT preprint CTP 723 (1978);
A.P. Contogouris, J. Kripfganz: McGill Univ. preprint, Montreal, Canada (1978)
8. B.L. Combridge: Phys. Rev. **D18**, 734 (1978)
9. J. Kripfganz, A. Schiller: Phys. Lett. **79B**, 317 (1978)
10. A.C. Hearn: REDUCE 2, Univ. of Utah, (1965)
11. F.A. Behrends, K.J.F. Gaemers, R. Gastmans: Nucl. Phys. **B63**, 541 (1973)
12. G. Sterman, S. Weinberg: Phys. Rev. Lett. **39**, 1436 (1977)
13. H. Georgi: Phys. Rev. Lett. **42**, 294 (1979)
14. J.F. Owens, E. Reya, M. Glück: Phys. Rev. **D18**, 1501 (1978);
J.F. Owens, E. Reya: Phys. Rev. **D17**, 3003 (1978)
15. J.H. Cobb et al.: Phys. Rev. Lett. **40**, 1420 (1978)

⁷ We used parton distribution functions of “counting rule types” proposed in [14]

⁸ Clearly, this is partly kinematical effect, so it must be true in a very broad class of models. The importance of fixing the transverse energy has been realized in the ISR experiment [15]

⁹ The enhancement is partly kinematical, so even a ratio > 1 does not mean necessarily that perturbation theory is not applicable